INTERNATIONAL COLLABORATION ON CO_2 SEQUESTRATION

Annual Report

Reporting Period: August 23, 2002 - August 23, 2003

Principal Authors:
Howard J. Herzog and E. Eric Adams

Issue date: March 2004

DOE Award No. DE-FG26-98FT40334

Massachusetts Institute of Technology
Energy Laboratory
77 Massachusetts Avenue
Room E40-455
Cambridge, MA 02139-4307
Telephone: (617) 253-0688
Fax: (617) 253-8013

Disclaimer

Abstract

The main goal of our work during this reporting period (August 23, 2002 – August 23, 2003) was to conduct an experimental cruise at the Loihi Seamount in the Hawaiian Islands. The work included preparation for the cruise, conducting the survey cruise, and analyzing the results. The cruise took place from December 3-13, 2002.

Table of Contents

Executive Summary

After the permit to conduct a field experiment in Norway was revoked on August 22, 2002, we started executing our contingency plan to conduct a cruise at the Loihi Seamount in Hawaii in December 2002. After a few intense months of preparation, the cruise took place on December 3-13, 2002. In total, eight dives were made with the Pisces V submarine. The primary goal of the experiment was to assess the effect of CO_2 on marine organisms. Studies were done using scavenger traps, as well as collecting water samples and surveying the natural CO_2 plume at the Loihi Seamount.

This report documents the experiment in more detail as summarized by the various participants. The data was still being analyzed at the end of this reporting period, so no results are reported here. Both papers and a video on the experiment are being prepared. Some related modeling work is presented in an Appendix in the form of a paper submitted to the Journal of Marine Environmental Engineering.

Experimental

From December 3-13, 2002, scientists from three countries representing the Technical Committee of the International Carbon Dioxide Sequestration Experiment examined the hydrothermal venting at Loihi Seamount (Hawaiian Islands, USA). Work focused on tracing the venting gases, the impacts of the vent fluids on marine organisms and their influence on biogeochemical cycles. The cruise on the R/V Ka'imikai-O-Kanaloa (KOK) included 8 dives of the Pisces V submarine, 6 at Loihi and 2 at a nearby site in the lee of the Big Island (Hawaii). Data gathered during the cruise will be published in peer-reviewed journals and will form the basis of grant proposals for future work at Loihi.

On the first dive two scavenger traps and two bait parcels (4 whole mackerel) were deployed, the vent fields were surveyed and water samples and real time CTD data including pH were obtained. The vent fields around HURL markers 35 and 37 were identified as likely sites for further work. According to the HURL Operations Manager Terry Kerby, recent changes in venting at Loihi included a near cessation of venting at the "Boiling Pot" site (previously venting at about 90°C), and at the "Jet Vent" site. During our cruise venting at marker 35 was broad and diffuse with temperatures at the seafloor as high as 31°C. Water with pH of 5.7 at 6.3°C was observed at marker 35. The vents at marker 37 were at the base of a cliff and included one large (about 30 cm) opening. The marker 35 vents were identified as the preferred site to expose trapped animals to the plume and the marker 37 site was determined to be best suited for plume surveys because of its more discrete source and proximity to a rock wall that could be used as a reference for the submersible.

On subsequent dives we conducted experiments on trapped animals and continued to take water samples, survey the plume, deploy traps and bait, and search for other nearby venting. Except for technological problems summarized below, the scavenger experiments went very well. We consistently trapped large numbers of amphipods (shrimp-like crustaceans) that were big enough to see clearly on video, and the plume used for testing ranged in pH from about 5.5-6.8 with

temperatures from about 4-6°C. Thus the animals suffered little thermal stress while being exposed to water highly enriched with carbon dioxide. During experiments the amphipods ceased swimming after 5-10 minutes in the plume and fell to the bottom of the trap (they continued to beat their respiratory appendages). Upon removal from the plume all or nearly all the animals revived within minutes. During ascent the animals remained quite active until the temperature reached 10-12°C at which point death appeared to occur rapidly. This confirmed that the reaction of the animals while in the plume was to some factor other than temperature.

During the 4th dive (PV-506, Dec 7h) strong trade winds resulted in high seas and the submarine was called to the surface while 20 minutes into the one-hour scavenger-plume experiment. The high seas at Loihi prevented diving for the next two days during which we dove in the lee of the Big Island, Hawaii. We examined the scavenging community at this site for comparison with Loihi and found a more diverse community, though we trapped only a fraction of the amphipods in 24 hours compared with Loihi.

Early in the cruise one bait parcel was placed within the vent fluids at both the marker 35 and 37 vents. Neither of these baits appeared to have been touched as of the last dive on Dec. 10 (PV-510). Baits deployed away from vents were largely consumed within 24 hours. Vent shrimp were observed on the bait in the vents and cutthroat eels (Synaphobranchidae) were attracted to the bait but refused to enter the plume that was made visible by shimmering water as vent and ambient water mixed.

The final two dives at Loihi were the key to the success of the cruise. It was during these dives that the best data were collected for the chemistry, bacteriological, and scavenger studies. Water column samples were taken primarily with the custom Niskin-style bottles mounted on the submersible (16 bottle rack). A few water samples in the plume were also collected using either a 3-liter Niskin sampler mounted on the front of the basket or a gas tight water sampler that could reach down into the vent by way of the manipulator arms. Analysis of bacteria included measurement of production and respiration to assess the variation in growth efficiency in and out of the plume. Chemical analyses included pH, DIC, alkalinity, salinity and stable and radiocarbon isotope analysis of DIC.

Technological problems hampered data collection throughout the cruise.
The acoustic release provided by HURL (the Hawaii Undersea Research Laboratory) needed to deploy the Acoustic Doppler Current Profiler (ADCP) malfunctioned and a replacement was delivered on the evening of Dec. 7th. Unfortunately high seas over the next two days prevented deployment of the current meter mooring.

The video system for the scavenger traps did not function properly, presumably because of a short-circuit that drained the battery in the 4 hours after the system was activated and before the submarine could dive, recover a trap, and transit to the site of venting. We compensated by using hand-held cameras through the submarines windows and ultimately by connecting our video camera to one of the Pisces V's recorders. This allowed us to obtain high quality video data but without crucial pH and temperature data. During two dives the CTD with the IOS pH probe was positioned under the scavenger trap to provide those data.

The water samplers were oriented vertically in a rack on the upper (forward) deck of the Pisces V. Because of the decking beneath the bottles they could only flush effectively if the vehicle was ascending and the presence of the submarine disrupted the vent plume during sampling. We also suffered from a lack of information on the water at the samplers when the bottles were tripped. These problems were ameliorated on the final dive by placing the CTD near the bottle rack and by sampling the plume obliquely to minimize disruption of the plume by the vehicle prior to sampling. A camera was also mounted for the last dive to view the tripping of the bottles as we had previously experienced many unsuccessful attempts to trip them making it difficult to determine where the samples had originated. Many of these "Niskin" bottles (custom made by HURL) also leaked upon surfacing, yielding little or no water.

Scientific Participants:
Hawaii Pacific University - Eric Vetter, Pierre Knutsson
University of Hawaii - Craig Smith, Sarah Minks
IOS - Keith Johnson, Magnus Eek
Naval Research Lab - Rick Coffin, Tom Boyd
DOE - Jeff Sommers
MIT - Eric Wannamaker
NIVA - Arild Sundfjord

Results and Discussion

The data is still being analyzed and will be reported in next year's report.

Conclusion

This cruise represents the 4th cruise undertaken by this experiment. Previous to this cruise, there were two survey cruises in Hawaii and one in Norway. Unfortunately, due to circumstances beyond the control of researchers in this project, we could never obtain a permit to inject CO_2 at depths greater than 500 m (see last year's report for more details). Therefore, this final cruise was used to study a natural CO_2 vent and investigate its affect on marine organisms. The data from this cruise is still being analyzed.

Despite the failure to obtain the permit, much knowledge was produced during this project via modeling studies, experimental studies, and the 4 cruises. Just under 100 technical papers and reports resulted either directly or indirectly from this project. A final report is now being prepared to document this effort.

References

None.

Appendix A:

Dilution Strategies for Direct Ocean Carbon Sequestration

E. Eric Adams and Eric J. Wannamaker

Department of Civil and Environmental Engineering
Massachusetts Institute of Technology
Cambridge, MA 02139 USA eeadams@mit.edu

ABSTRACT

Ocean carbon sequestration has been mentioned as one approach to help address global climate change. Among the issues requiring consideration is the need to obtain high initial dilution, in order to minimize the excess concentrations of dissolved inorganic carbon, and hence associated increases in pCO_2 and decreases in pH, to which aquatic life would be exposed. Here we examine three dilution strategies that promote mixing in the longitudinal, lateral and vertical directions. A point release of negatively buoyant solid CO_2 hydrate particles from a moving ship would get acceptable dilution near the source, while subsequent concentrations would be very low due to longitudinal mixing afford by the ship's speed. A long bottom-mounted diffuser discharging buoyant liquid CO_2 droplets can be designed for high lateral mixing, resulting in arbitrarily small near source concentrations, but because the resulting near field plume would be very wide, subsequent dilution would be slow. A stationary point release of hydrate particles achieves good vertical mixing, due to the negatively buoyant plume effect, resulting in intermediate local and subsequent concentrations. While directly applicable to ocean carbon sequestration, results presented here also provide guidance for the effective three-dimensional dispersal of other tracers, such as nutrients for open water aquaculture, or flocculants or algaecides for improving water clarity in reservoirs or town ponds.

Keywords: ocean carbon sequestration, CO_2 plume, CO_2 hydrate, ocean dispersion, dilution

INTRODUCTION

Atmospheric CO_2 concentrations have been increasing since the industrial revolution, due in large part to increased fossil fuel combustion. Because CO_2 is a greenhouse gas, the increasing concentrations have generated concern about global climate change. One suggestion to address global change is to capture CO_2 from stationary power sources and pump it directly into the ocean, by-passing the slower biological and solubility pumps by which approximately 80 percent of the carbon dioxide that we currently emit to the atmosphere will ultimately invade the ocean (Herzog et al., 2001). The time scale of ocean circulation would limit the benefits of such mitigation to a few centuries (Orr et al., 2001), but since this time frame exceeds the expected duration of fossil fuel use, it could serve to reduce both peak atmospheric concentrations and their rate of increase (Kheshgi, 2002), both of which have been shown to affect the magnitude of climate response (Stocker & Schmittner, 1997). Eventually (on a time scale of millennia), the concentration in the atmosphere and ocean will reach an equilibrium that is independent of where the CO_2 was released (Herzog et al. 2001).

Ocean sequestration can only be considered viable if the resulting impacts to the marine environment are small in comparison with the avoided impacts associated with climate change. Acute effects--hypercopnia, (caused by elevated levels of pCO_2) and respiratory stress and acidosis (caused by associated lowering of pH)--could be experienced by individual organisms unable to avoid the plume (Knutzen, 1981; Shirayama, 1997; Omori, et al., 1998, Tamburri, et al., 2000). Additional sub-lethal effects could occur at the community and ecosystem level (Portner and Reipschlager, 1996; Kita et al., 2002). Both will depend on the duration as well as the magnitude of exposure (Auerbach, et al., 1997; Watanabe, et al., 2002). Concentrations near the source will be highest, and most variable, but also most dependent on the method of injection, which can be controlled. At regional and global scales, concentrations will depend on the magnitude and the locations of release, and less on the method of release. In this paper we focus on the near source impacts and their sensitivity to the method of injection.

While directly applicable to ocean carbon sequestration, results presented here also provide guidance for the effective 3-dimensional dispersal of other tracers, such as nutrients for open water aquaculture, or flocculants or algaecides for improving water clarity in reservoirs or town ponds.

INJECTION SCENARIOS

From the above discussion it is clear that one strategy for a CO_2 injection scheme is to produce initial mixing, thereby creating low near-source perturbations in concentrations and pH. Injection schemes to induce mixing can be categorized in terms of the spatial dimension over which they initially spread the CO_2. A continuous point release achieves significant spread in the vertical direction by virtue of the plume buoyancy, which can be either positive or negative, depending on the phase of the CO_2 and the depth of release. A release from a ship-based towed pipe achieves spreading in the longitudinal direction (parallel to the ship's motion). Finally, a stationary manifold mounted either on the sea-floor or suspended in the water column could induce spreading in the lateral direction (perpendicular to a prevailing ambient current).

Table 1 is a matrix of possible CO_2 injection methods based on buoyancy and the dilution options listed above. For each type of release a preference is indicated. For a single plume release, negative buoyancy is preferred as it yields a deeper sequestration depth, and greater sinking (hence dilution), than an equivalent buoyant release (see following discussion). For a towed pipe release, negative buoyancy is preferred because it yields a deeper sequestration depth. Finally, a sea-floor mounted manifold injecting positively buoyant CO_2 is preferred, because a manifold-based release of negative buoyancy is impractical.

Table 1: Options for ocean CO_2 injection. Preferred options indicated with an X

	Single Plume	Towed Pipe	Manifold
Positive Buoyancy			X
Negative Buoyancy	X	X	

The following sections compare the preferred techniques in terms of the excess concentration of dissolved inorganic carbon (DIC) and hence the change in pH, using as measures the average pH shift as a function of distance (or time of travel) and the volume of water in a given pH range. The comparison assumes as a base case, a CO_2 injection rate of 100 kg/s (the approximate release from a 500 MW coal plant; Herzog et al., 1991), a release depth of 800 m, a total water depth of 4500 m, a uniform ambient current of 5 cm/s, a common ambient density profile (**Figure 1**), and a common lateral mixing parameterization (explained below). Model sensitivity to these variables is also discussed.

Sinking CO_2 hydrate plume

The strategy of a sinking plume is to release CO_2 relatively near the surface, but have it sink to greater depths. The sinking aids sequestration, since the CO_2 is placed deeper in the water column, and numerical model studies show a strong correlation between sequestration time and (effective) depth of injection (Orr, et al., 2001). Many ways have been proposed to create a sinking plume. Dry ice (Nakashiki et al., 1994, Caulfield 1996) and very cold liquid CO_2 (Aya et al., 1999) are negatively buoyant phases of pure CO_2. CO_2 can be made to react with $CaCO_3$ to form dense $CaCO_3$ slurries (Caldeira and Rau 2000), or put into a $CaCO_3$ emulsion (Golomb 2002). A highly concentrated CO_2 and seawater solution is negatively buoyant and may be used to induce a gravity current (Haugan and Drange, 1992, Adams et al 1995, 1997, Saito et al. 2000). And at depths below about 500 m, CO_2 will form a negatively buoyant clathrate hydrate ($CO_2 \bullet nH_2O$, Holder et al. 2001). Most of these scenarios involve multiple CO_2 phases. For example, with CO_2 hydrates, the CO_2 is released as negatively buoyant solid particles (SG $\approx$ 1.1) that sink as they dissolve. The CO_2-ennriched seawater that results from dissolution is also

negatively buoyant, leading to greater sinking. For a given mass delivery rate, greater sinking means the CO_2 is spread over a greater vertical interval, which increases the dilution, leading to lower excess concentrations of CO_2 and changes in pH. Wannamaker (2002) and Wannamaker and Adams (2004) show that a negatively buoyant solid hydrate plume will sink up to twice as far as an equivalent positively buoyant hydrate plume will rise. It should be noted that it is difficult to produce a pure hydrate plume, and that efforts-to-date have resulted in only partial hydrate formation; however, even plumes formed with partially hydrated particles have exhibited significant sinking (Lee, et al., 2003).

Figure 2 shows a schematic of the hydrate plume release. Wannamaker (2002) and Wannamaker and Adams (2004) show that particle diameter and mass loading are the major design variables influencing plume characteristics, while the rate of hydrate dissolution is a major uncertain parameter. For the purposes of comparison, we assume that 354 kg/s of solid CO_2 hydrates (100 kg/s CO_2 for a hydrate number of $n = 6$) are released in the form of 2.5 cm diameter solid particles. As modeled, this release spans the entire water column without allowing any un-dissolved mass to reach the bottom.

Dilution for a CO_2 hydrate plume is based on the negatively buoyant plume model of Wannamaker (2002) and Wannamaker and Adams (2004), which is a modification of the integral double plume model applied to positively buoyant plumes by Crounse (2000) and Crounse et al. (2004). For negatively buoyant plumes, the dispersed phase (i.e., solid CO_2 hydrates) and associated entrained water are modeled as a sinking inner plume, while the counter flowing intrusions created from peeling events are modeled as an outer plume. Plume evolution is described by entrainment fluxes of water, momentum, salt, heat and dissolved CO_2 from the ambient to the outer plume, from the outer to the inner plume and vice versa, and detrainment from the inner plume as indicated in **Figure 3.**

The integral plume model strictly applies to quiescent receiving water, but should give approximately valid calculations for weak crossflows—defined as ambient currents with insufficient magnitude to cause the dispersed and continuous plume phases to separate for a given particle slip velocity and ambient stratification profile. Using relationships for phase

separation described in Socolofsky and Adams (2002), Wannamaker and Adams (2004) show that for the modeled stratification (Figure 1), and an initial hydrate particle diameter of 2.5 cm or less, an ambient current of 5 cm/s will be considered "weak" for CO_2 mass loadings greater than about 20 kg/s, hence justifying the chosen modeling approach.

A sub-model controls the dissolution of CO_2 from the dispersed phase, which becomes a source of dissolved CO_2 for the inner model. A standard mass transfer model is modified to apply to solid hydrate particles:

$$\frac{dM_h}{dt} = -\lambda AKC_s \frac{MW_{hyd}}{MW_{CO_2}} \tag{1}$$

where M_h is the mass of a spherical CO_2 hydrate particle, A is its surface area, K is a mass transfer coefficient that depends on the droplet size and velocity (Clift et al., 1978), C_s is the surface concentration which equals the solubility of CO_2 in the ocean, and the ratio of molecular weights of hydrate and pure CO_2 is about 3.5. λ is an empirical mass transfer inhibition factor that accounts for the slower dissolution rate of hydrates relative to pure CO_2. Based on field data from Rehder et al. (2001), Wannamaker (2002) and Wannamaker and Adams (2004) identified $\lambda \cong 0.19$.

In order to extend results beyond the near field influence of the plume, a simple relative diffusion model has been included. Okubo (1971) describes the evolution of instantaneously released dye patches versus time in coastal surface waters. Assuming diffusion properties at depth are similar to those in coastal surface waters, Okubo's data can be applied to the lateral spread of a continuous plume of finite initial width following

$$\sigma_y = a(t_o + t)^n \tag{2}$$

with $a = 7.1 \times 10^{-4}$ and n = 1.15, where σ_y is the lateral standard deviation of plume concentration in m, t is elapsed time in seconds, and t_o is an initial time corresponding to the finite initial plume

width, computed from Eq. 2 using t = 0 and $\sigma_{y,0} = \dot{m} / 3hDIC_o u_a$, where $\dot{m}$ is the CO_2 mass loading rate, the initial plume thickness h is taken as the computed near field plume height, the initial concentration DIC_o is taken as the computed depth-average plume concentration, and u_a is the ambient current speed. That is,

$$t_o = \left(\frac{\dot{m}}{3hDIC_o u_a a} \right)^{1/n} \tag{3}$$

The model ignores vertical diffusion given that the vertical mixing time scale of h^2/E_z is much greater than the lateral mixing time scale of w^2/E_y with $E_y \approx 10^3 E_z$. The average excess carbon concentration is then calculated as

$$DIC_{ave} = \frac{\dot{m}}{3\sigma_y(t) h u_a} \tag{4}$$

from which pH can be calculated based on typical ocean alkalinity (Wannamaker, 2002). The solid line in **Figure 4** shows pH as a function of time up to 10 hours (corresponding to a downstream distance of 1.8 km based on a current speed of 5 cm/s).

Another measure of impact is the volume of water at different pH levels produced by the plume. With the excess DIC cloud approximated as a Gaussian distribution as above, excess DIC concentration can be calculated as function of time and lateral distance, y:

$$DIC(t, y) = \frac{\dot{m}}{\sqrt{2\pi} h u_a \sigma_y(t)} \exp\left[\frac{-y^2}{2\sigma_y{}^2} \right] \tag{5}$$

where $\sigma_y(t)$ is calculated as described previously. Eq. 5 may be solved for the lateral coordinate of a given excess DIC concentration:

$$y = \sigma_y(t)\sqrt{-2\ln\frac{DIC}{C_c(t)}} \tag{6}$$

where the plume centerline concentration is given by

$$C_c(t) = \frac{\dot{m}}{\sqrt{2\pi}hu_a\sigma_y(t)} \tag{7}$$

Eq. 6 allows the width of a given concentration contour, $b = 2y$, to be calculated for each time. The volume of water with concentration greater than or equal to a given excess DIC concentration is then:

$$V(DIC) = h\int_0^x b(x'/u)dx' \tag{8}$$

where the equation is framed in terms of downstream distance, x, by substituting t = x/u. Eq. 8 can be solved numerically for a few values of DIC. The solid line in **Figure 5** shows the predicted volume of water at different ranges of pH drop produced by a CO_2 hydrate plume. There is a large volume of water produced in the fairly low pH drop range from 0.1 to 0.5 units. A comparatively smaller volume of water is produced with impact greater than 0.5 pH units.

CO_2 hydrate particles released from a moving ship

A ship-based release is envisioned as a towed pipe releasing 354 kg/s of CO_2 hydrates (100 kg/s of CO_2) at a depth of 800 m. The ship velocity, set at 3 m/s, is a possible design variable to optimize dilution. Mixing induced by the pipe, analyzed by Tsushima et al. (2002) for a liquid CO_2 injection, is ignored because hydrate particles would sink below the pipe, unlike positively buoyant CO_2 droplets. The ship trajectory is assumed to be straight, perpendicular to the prevailing current, and infinite in extent. **Figure 6** shows the release schematically.

The particle sinking depth is calculated based on isolated, falling particles with a mass transfer model as presented earlier, except with the ambient current velocity of 5 cm/s included in the magnitude of velocity used for the mass transfer coefficient correlations. Note that, due to drag, the particles move at the ship velocity for a negligible amount of time, so that the ship velocity does not affect particle dissolution. For an initial particle diameter of 2.5 cm, the predicted dissolution depth below release is h=1390 m. The fact that this depth is less than 40% of the dissolution depth for a sinking CO_2 hydrate plume reflects the absence of a plume effect. For purposes of dilution modeling, particle dissolution is assumed to take place uniformly over this depth, resulting in a uniform vertical concentration distribution. A Gaussian lateral concentration distribution is assumed, resulting in a peak initial excess DIC concentration of

$$DIC_o = \frac{\dot{m}}{\sqrt{2\pi}\sigma_{y,0} h U_s} \tag{9}$$

where the initial standard deviation, $\sigma_{y,0}$, is taken as 0.1 m. Downstream from the release, the average excess DIC concentration as a function of time can be calculated as before:

$$DIC_{ave}(t) = \frac{\dot{m}}{3\sigma_y(t) h U_s} \tag{10}$$

where U_s is the velocity of the ship, and $\sigma_y(t)$ is calculated from Eq. 2. The dashed line in Figure 4 shows the predicted average pH drop traveling away from the ship, or at a stationary point, depending on the frame of reference. The pH drop is initially significant due to the low initial dilution, but falls close to ambient levels quickly due to the large value of U_s.

The volume of water in different pH ranges can be calculated similarly to the method used for a hydrate plume, with the exception that U_s is substituted for u_a. This yields the predictions shown by the dashed lines in Figure 5. Although there is some volume of water at the high pH drops, a comparatively larger volume of low impact water is produced.

Rising CO_2 droplets released from a bottom manifold

A bottom manifold release could be achieved with a pipeline extending on the sea-floor to a depth of 800 m and beyond. The pipeline is modeled as perpendicular to the uniform ambient current of 5 cm/s, and 100 kg/s of liquid CO_2 would be injected through a number of equally spaced ports. At a depth of 800 m, liquid CO_2 is about 10% less dense than ambient seawater, so the buoyant CO_2 from each port would produce rising plumes that would ultimately merge. For modeling purposes, the height of the plumes, h, and the length of the manifold, L, are considered design variables. In other words, it is assumed that droplet size and individual diffuser mass flux can be varied to spread the CO_2 evenly over a given h and L, within reasonable limits. In practice, for a release at 800 m, h is limited to about 400 m due to the volatilization of CO_2 at about 400 m depth, whereas L might be constrained by pipeline cost. A value of 250 m is taken for h as a compromise between sequestration depth and dilution. L is taken as half of the pipeline length required to reach 800 m, L_o. For an assumed sea-floor slope of $\theta = 5$ degrees, L_o is about 9000 m; therefore, L is taken as 4500 m. Following Crounse (2000), CO_2 plumes discharged over a bottom manifold of length L = 4500 m, and dissolving over a height of h = 250 m, could be obtained using 100 ports, each discharging 1 kg/s of CO_2 with an initial droplet diameter of about 0.7 cm. This assumes that the CO_2 droplets are covered with a thin hydrate film, that results in a factor of two reduction in the rate of mass transfer, as compared with liquid CO_2 (Hirai, et al., 1997). **Figure 7** depicts a sea-floor manifold release schematically.

The manifold system results in a rectangular source of height h, length L, and uniform initial excess DIC concentration,

$$DIC_o = \dot{m} / Lhu_a \tag{11}$$

Subsequent lateral diffusion of the resulting cloud is based on an initial width, w = h/tanθ or L, whichever is smaller. (See Figure 7.) The downstream distribution of DIC is modeled using a finite width and depth plane source without vertical diffusion:

$$DIC(y,t) = \frac{\dot{m}}{2Lhu_a}\left[erf\left(\frac{y+w/2}{\sqrt{2}\sigma_y(t)}\right) - erf\left(\frac{y-w/2}{\sqrt{2}\sigma_y(t)}\right)\right] \quad (12)$$

where $\sigma_y(t)$ is calculated from Eq. 2, with an initial value of w/3. An approximate average concentration as a function of time downstream is given as $DIC_{ave}(t) \cong DIC_o\sigma_{y,0}/\sigma_y(t)$ or, assuming h/tanθ < L,

$$DIC_{ave} \cong \left(\frac{\dot{m}}{Lu_a}\right)\left(\frac{1}{3\tan\theta\sigma_y(t)}\right) \cong \left(\frac{\dot{m}}{Lu_a h}\right)\left(\frac{1}{1+\left(\frac{3a\tan\theta}{h}\right)^{1/n}t}\right)^n \quad (13)$$

The dot-dash line in Figure 4 shows the average concentration as a function of time traveling downstream form the manifold. The manifold achieves high initial dilution, but it takes a long time to achieve much additional dilution beyond that. A zero solving scheme is used to get the volume in different pH ranges from Eq. 12. As indicated by the dot-dash line in Figure 5, this yields a volume of about 1.4 km^3 of water between a pH drop of 0.5 and 0.1 after ten hours.

Base case summary

Figure 4 compares the three discharge strategies in terms of average pH drop. Generally, the towed pipe and the hydrate plume create the highest initial pH impact, but both are able to achieve good dilution within ten hours, with the towed pipe benefiting more from lateral dilution, because of its narrower initial width. The sea-floor mounted manifold achieves a low near field pH impact, but doesn't benefit much from lateral dilution due to its large, uniform, initial concentration field. Overall, the towed pipe method yields the lowest pH impact after ten hours.

Figure 5 shows the volumes in different ranges of pH change for each method. The towed pipe shows the most potential for acute (high pH change) impacts due to its relatively low initial mixing, but the impacted volume would be very small. The sea-floor mounted manifold

could present a higher danger for chronic impact, based on its large volume in the lowest pH shift rang. The hydrate plume represents a compromise between the other two cases.

ADDITIONAL DISCUSSION

Qualitative sensitivity analysis

The initial excess concentrations associated with each scenario can be expressed as

$$DIC_o \sim \frac{\dot{m}}{h\sigma_{y,o}U} \tag{14}$$

where the characteristic depth h, width $\sigma_{y,0}$, and velocity U differ among scenarios. The downstream excess concentration reflects additional lateral diffusion. Based on Eq. 2, the additional dilution depends on the initial time t_o corresponding to the initial plume width, $\sigma_{y,0}$, or

$$DIC_{ave}(t) \sim \frac{\dot{m}}{h\left[\left(\frac{\sigma_{y,0}}{a}\right)^{1/n} + t\right]^n U} \tag{15}$$

where, depending on the scenario, Eq. 14 may be used to express $\sigma_{y,0}$ in terms of initial concentration. The relationship among characteristic depth, width and velocity for the three scenarios is depicted schematically in **Figure 8**.

Sensitivity to mass loading, initial particle/droplet size and site depth. In all three scenarios, concentrations are nominally proportional to the mass loading, but for the sinking hydrate plume, an increase in mass loading (and hence plume buoyancy) leads to an increase in both the plume depth and the rate of entrainment per unit depth, and hence to an increase in plume width. Indeed, Wannamaker (2002) and Wannamaker and Adams (2004) found that an increase in $\dot{m}$ of three orders of magnitude resulted in only a four-fold increase in initial excess

concentration, as a consequence of the increase in plume depth and width. Plume depth is also dependent on initial particle diameter, suggesting that, all else equal, larger particles (or smaller rate of mass transfer) will produce smaller concentrations. However, the finite depth of the ocean places a natural limit on the dilution from a point source: any undissolved hydrate particles reaching the seafloor will accumulate in a mound that will dissolve, but at a slower rate than the descending particles (Wannamaker, 2002). It follows that dilution with this injection scenario can be maximized by locating the release in deep water.

For a moving ship, the hydrate particles fall independently, so there is no plume effect to cause an increase in depth with increasing mass loading. However, like the sinking hydrate plume, the depth of dissolution increases with increasing particle size (or decreasing mass transfer rate), suggesting the desirability of large initial particles released at deep sites. For buoyant plumes emanating from a bottom manifold, Crounse (2000) shows that plume height h increases modestly with mass loading, and significantly with increasing droplet diameter. Since the plume must be confined to a vertical interval between the local water depth, and a depth of about 400 m below the surface (at which a liquid-gas phase change occurs), releases with relatively large droplets at deep sites are preferable.

Sensitivity to lateral diffusion Diffusion is the dominant process affecting downstream dilution. As indicated in Eqs. 2 and 15, diffusion depends on the initial time t_o and hence the initial source size. It follows that for lateral diffusion to be significant, time t must be at least comparable with t_o. It is therefore helpful to compare the magnitudes of the equivalent initial timescales for the three releases, as they are depicted in Figure 8. For the sinking hydrate plume (point source) the initial lateral size is on the order of ten meters. This gives an initial equivalent timescale of order 1000 sec, indicating that lateral diffusion becomes important rather quickly. The towed pipe release as modeled has an even smaller initial size of order 0.1 m, corresponding to a timescale of order 100 sec, so lateral diffusion becomes important almost immediately. Conversely, the manifold type release has an initial size of thousands of meters, giving an equivalent initial time scale of several days, resulting in very little additional dilution. As indicated in Figure 7 and Eq. 13, the initial source size is inversely proportional to the bottom slope, suggesting that deep sites produce better dilution (they also require shorter pipes).

Although the manifold scenario does not achieve much additional dilution, there is consolation in the fact that dilution is a function of design and not (uncertain) environmental parameters.

Sensitivity to current speed. The role of an ambient current is to spread out the plume and, in some cases, provide dilution; hence there may be effects for both initial and downstream dilution. Because of the strong plume effect caused by the concentrated source of negative buoyancy, initial dilution for the sinking hydrate plume is independent of current speed, but downstream dilution increases with increasing current because, all else equal, a strong ambient current generates a smaller initial source width, as shown in Eq. 3. In the analysis for the towed ship, the ship speed replaces the ambient current speed. Thus, while both initial and subsequent dilution are independent of the ambient current, they are linearly dependent upon ship speed. Hence the largest practical ship speed should be considered. For the bottom manifold, both the initial and subsequent dilution are directly proportional to ambient current.

Quantitative Sensitivity Analysis

The above analysis suggests that the three scenarios are affected primarily by two ambient variables (diffusion and current speed) and two design variables (mass loading rate and initial hydrate/droplet diameter). Table 2 shows how each of these variables affects initial concentrations and downstream concentrations. The downstream concentration is evaluated at a nominal time of 5.4 hours after release, which corresponds to a downstream distance of 1000 m in a 5 cm/s current. The analysis was performed by considering a three-fold change in each independent variable in the direction that causes an increase in concentration (i.e., decreasing the diffusivity parameter a, the ambient current and the hydrate/particle size, and increasing the CO_2 loading) and noting the percentage change in concentration.

Table 2: Percentage increase in initial concentration (top) and downstream concentration (bottom) as a result of a three-fold decrease in lateral diffusion, ambient current and initial diameter and a three-fold increase in mass loading.

	Lateral Diffusion	Ambient Current	Mass Loading	Initial Diameter
Hydrate Plume	0 160	0 160	40 120	80 130
Towed Pipe	0 200	0 0	200 200	100 100
Bottom Manifold	0 6	200 200	200 200	0 0

CONCLUSIONS

Three distinctly different scenarios have been analyzed for their ability to disperse CO_2 over wide volumes of the ocean, for purposes minimizing the near field impacts associated with direct ocean sequestration. Our analysis indicates that any of the three techniques can achieve reasonable dilution if designed properly. The towed ship technique is the most desirable for reaching ambient pH levels quickly, while the sea-floor manifold provides the most near field dilution. The three techniques are also sensitive to ambient parameters, but in different ways. For example dilution from the towed pipe is sensitive to ambient diffusivity, but not to current, while dilution from the bottom manifold is directly proportional to ambient current, but relatively insensitive to ambient current,

ACKNOWLEDGMENTS

Eric Wannamaker received financial support through a National Science Foundation graduate research fellowship. Additional support was provided by the Ocean Carbon Sequestration

Program, Biological and Environmental Research (BER), U.S. Dept of Energy (grant number DE-FG02-01ER63078); and the National Energy Technology Laboratory, U. S. Dept. of Energy (grant number DE-FG26-98FT40334).

REFERENCES

Adams, E.E., D. Golomb, X.Y. Zhang, & H.J. Herzog, (1995), "Confined release of CO_2 into shallow sea water", in *Direct Ocean Disposal of Carbon Dioxide*" TERRAPUB, Tokyo, pp 153-164.

Adams, E., Caulfield, J. & Zhang, X. (1997) "Sinking of a CO_2-enriched ocean gravity current." *Proc. 27th IAHR Congress*: 352-357, San Francisco.

Auerbach, D., J. Caulfield, E. Adams & H. Herzog, (1997) "Impacts of ocean CO_2 disposal on marine life: I. A toxicological assessment integrating constant-concentration laboratory assay data with variable-concentration field exposure", *Environmental Modeling and Assessment* 2: 333-343.

Aya, I., K. Yamane, & K. Shiozaki, (1999), "Proposal of self-sinking CO_2 sending system: COSMOS", *Proc GHGT-4 Conference:* 269-274.

Caldeira, K. & G.H. Rau, (2000), "Accelerating carbonate dissolution to sequester carbon dioxide in the ocean: Geochemical implications", *Geophysical Research Letters* 27(2): 225-228.

Caulfield, J.A. (1996), "Environmental impacts of carbon dioxide ocean disposal: plume predictions and time-dependent organism experience" MS thesis, Dept of Civil & Environmental Engineering, MIT. Cambridge, MA.

Clift, R., J.R. Grace, & M.E. Weber, (1978), *Bubbles, Drops and Particles*, Academic Press, New York, NY.

Crounse, B.C., (2000) "Modeling buoyant droplet plumes in a stratified environment", MS thesis, Dept. of Civil and Environmental Engineering, MIT, Cambridge, MA.

Crounse, B.C., E. J. Wannamaker, & E. E. Adams, (2004), "Integral model of a multi-phase plume in quiescent stratification" submitted to *Journal of Hydraulic Engineering*.

Golomb, D. (2003), "Carbon dioxide/limestone/water emulsion for ocean and geological sequestration of CO_2", *Greenhouse Gas Control Technologies (Proc 6th Int'l Conf on Greenhouse Gas Control Technologies)*, Elsevier Science, Ltd., Kidlington, Oxford, UK: 683-688.

Haugan, P. & H. Drange, (1992), "Sequestration of CO_2 in the Deep Ocean by shallow injection", *Nature* 357(28): 1065-1072.

Herzog, H., J., D.S. Golomb, & S. Zemba, (1991), "Feasibility, modeling and economics of sequestering CO_2 emissions in the deep ocean", *Environmental Progress* 10(1): 64-74.

Herzog, H, K. Caldeira, & E. Adams, (2001), "Carbon sequestration via direct injection, in J. Steele, S. Thorpe & K. Turekian, eds, *Encyclopedia of Ocean Sciences*, Vol 1, Academic Press, London, pp. 408-414.

Hirai, S., K. Okazaki, Y. Tabe, K. Hijikata, & Y. Mori, (1997), "Dissolution rate of liquid CO2 in pressurized water flows and the effect of clathrate films", *Energy* 22(2/3): 285-293.

Holder, G., L. Mokka, & R. Warzinski, (2001), "Formation of hydrates from single –phase aqueous solutions and implications for ocean sequestration of CO_2", *Preprints, Spring 2000 National Meeting, ACS Division of Fuel Chemistry*, San Diego, CA.

Kheshgi, H., (2003) " Evasion of CO_2 injected into the ocean in the context of CO_2 stabilization", *Greenhouse Gas Control Technologies (Proc 6th Int'l Conf on Greenhouse Gas Control Technologies)*, Elsevier Science, Ltd., Kidlington, Oxford, UK:811-816.

Kita, J. Ishimatsu, A., Kikkawa, T. & Hayashi,M.. (2003), "Effects of CO_2 on marine fish", *Greenhouse Gas Control Technologies (Proc 6th Int'l Conf on Greenhouse Gas Control Technologies)*, Elsevier Science, Ltd., Kidlington, Oxford, UK: 1695-1698.

Knutzen, (1981), "Effects of decreased pH on marine organisms", *Marine Pollution Bulletin* 12:25-29.

Lee, S.L., L. Liang,, D. Riestenberg, O.R. West, C. Tsouris, & E. Adams, (2003) "CO_2 hydrate composite for ocean carbon sequestration" *Environmental Science and Technology* 37:3701-3708.

Nakashiki, N., T. Ohsumi, & K. Shitashima, (1994), "Sequestering of CO_2 in a deep ocean", *Technical Report*, Central Research Institute of Electric Power Industry, Abiko-City, Japan.

Okubo, A. (1971), "Oceanic diffusion diagrams", *Deep Sea Research* 18:789-802.

Omori, M., C.P. Norman, & T. Ikeda, (1998), "Oceanic disposal of CO2: potential effects on deep-sea plankton and micronekton—a review", *Plankton Biol. Ecol*. 45:87-99.

Orr, J.C., O. Aumont, A. Yool, K. Plattner, F. Joos, E. Maier-Reimer, M-F Weirig, R. Schlitzer, K. Caldeira, M. Wickett & R. Matear., (2001) "Ocean CO2 sequestration efficiency from 3-D ocean model comparison", Greenhouse Gas Control Technologies (*Proc 5th Int'l Conf on Greenhouse Gas Control Technologies*), CSIRO Publishing, Collingwood, VIC, Australia.

Portner, H-O & A. Reipschlager, (1996), "Ocean disposal of anthropogenic CO_2: physiological effects on tolerant and intolerant animals". In *Workshop 2-Environmental Impact*. IEA Greenhouse Gas R&D Programme, Cheltenham, UK, pp 57-81.

Rehder, G., S.H. Kirby, W.B. Durham, L. Stern, E.T. Peltzer, & J. Pinkston, (2001), "Dissolution rates of synthetic methane hydrate and carbon dioxide hydrate in undersaturated seawater at 1000m depth". Monterey Bay Aquarium Research Institute, Moss Landing, CA.

Saito, T., T. Kajishima, & R. Naguosa, (2000), "CO_2 sequestration at sea by gas-lift system of shallow injection and deep releasing", *Environmental Science and Technology* 34, 4140-4145.

Shirayama, Y., (1997), "Biodiversity and biological impact of ocean disposal of carbon dioxide," *Waste Management* 17:381-384.

Socolofsky, S.A. & E.E. Adams, (2002), "Multi-phase plumes in uniform and stratified crossflow", *Journal of Hydraulic Research* 40(6):661-672.

Stocker, T.F. & S. Schmittner, (1997), "Influence of CO_2 emission rates on the stability of the thermohaline circulation", *Nature* 388:862:865.

Tamburri, M.N., E.T. Peltzer, G. E. Friederich, I. Aya, K. Yamane & P. Brewer, (2000), "A field study of the effects of CO2 ocean disposal on mobile deep-sea animals", *Marine Chemistry* 72:95-101.

Tsushima, S., S. Hirai, H. Sanda & S. Terada, (2003), "Experimental studies of liquid CO_2 injection with hydrate film and highly turbulent flows behind releasing pipe", *Greenhouse Gas Control Technologies (Proc 6th Int'l Conf on Greenhouse Gas Control Technologies)*, Elsevier Science, Ltd., Kidlington, Oxford, UK.:837-842.

Wannamaker, E. J. (2002), "Modeling carbon dioxide hydrate particle releases in the deep ocean" MS thesis, Dept of Civil & Environmental Engineering, MIT. Cambridge, MA.

Wannamaker, E.J. & E. E. Adams (2004), "Modeling descending carbon dioxide injections in the ocean" submitted to *Journal of Hydraulic Research*.

Watanabe, Y., A. Yamaguchi, H. Ishida, T. Ikeda & J. Ishizaka, (2003), "Lethal effect of elevated pCO_2 on planktons collected from deep sea in North Pacific", *Greenhouse Gas Control Technologies (Proc 6th Int'l Conf on Greenhouse Gas Control Technologies)*, Elsevier Science, Ltd., Kidlington, Oxford, UK: 1683-1686.

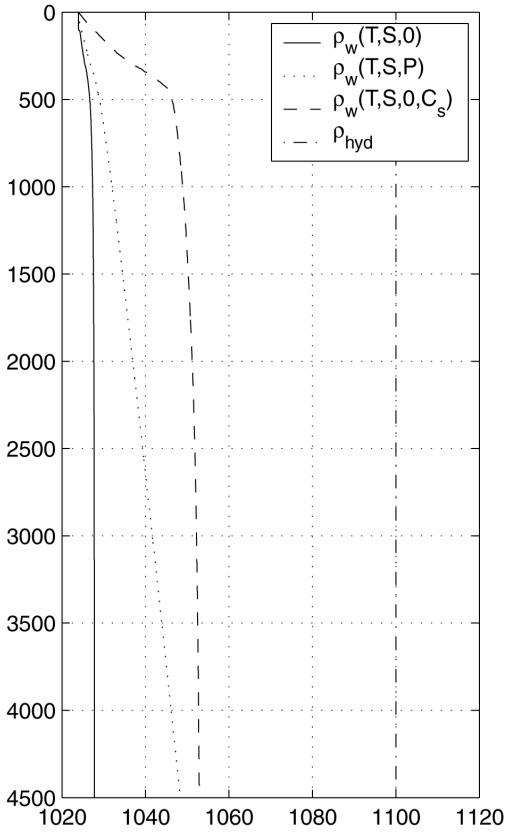

Figure 1 Ambient density profile used in model simulations

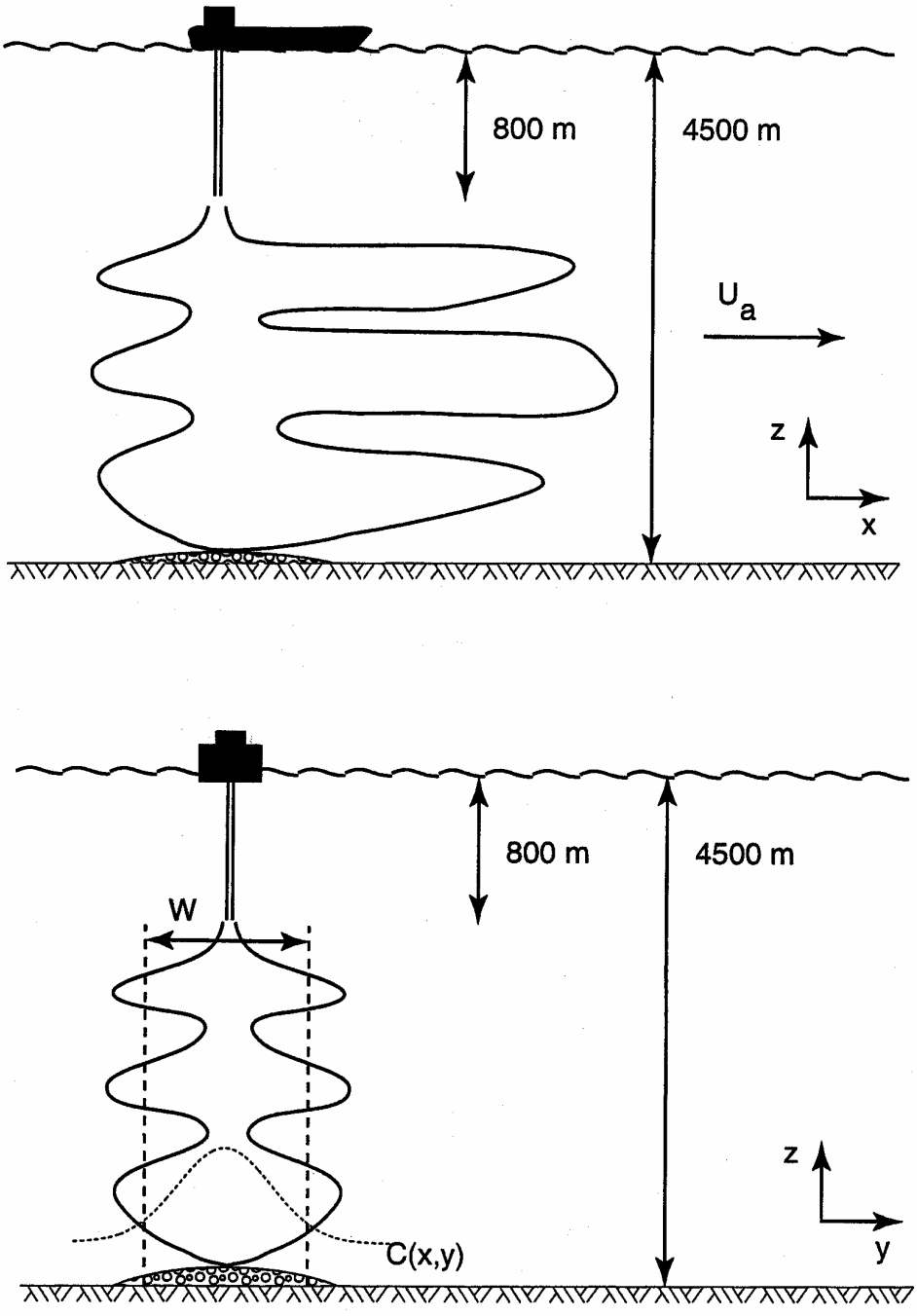

Figure 2 Sinking CO_2 hydrate plume formed from a stationary point source

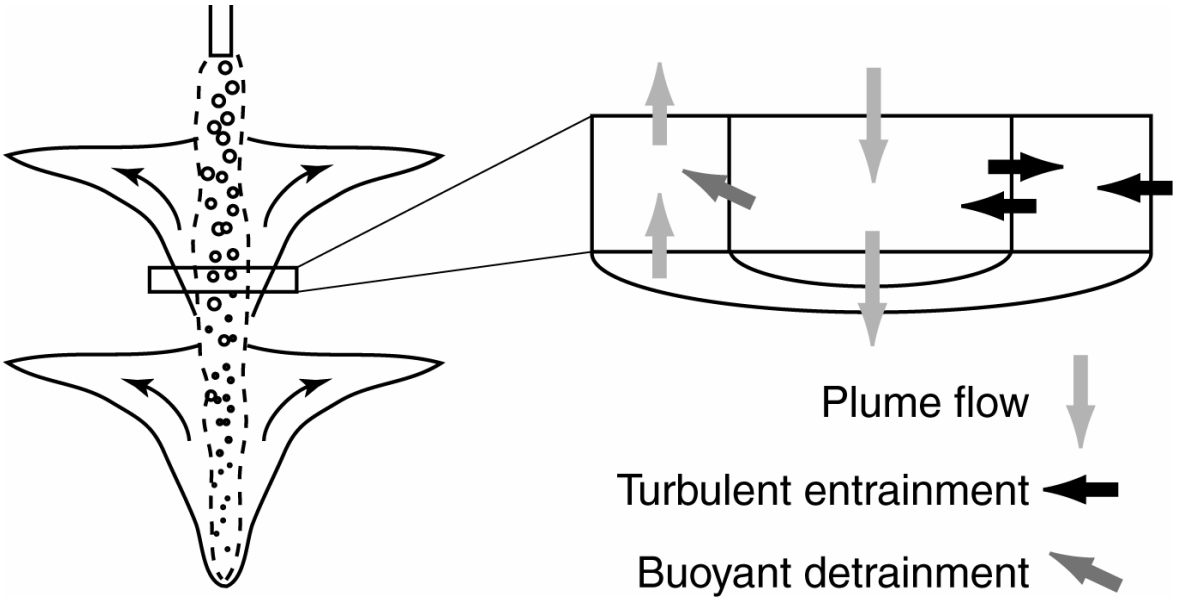

Figure 3 Double plume model used to analyze negatively buoyant hydrate plumes

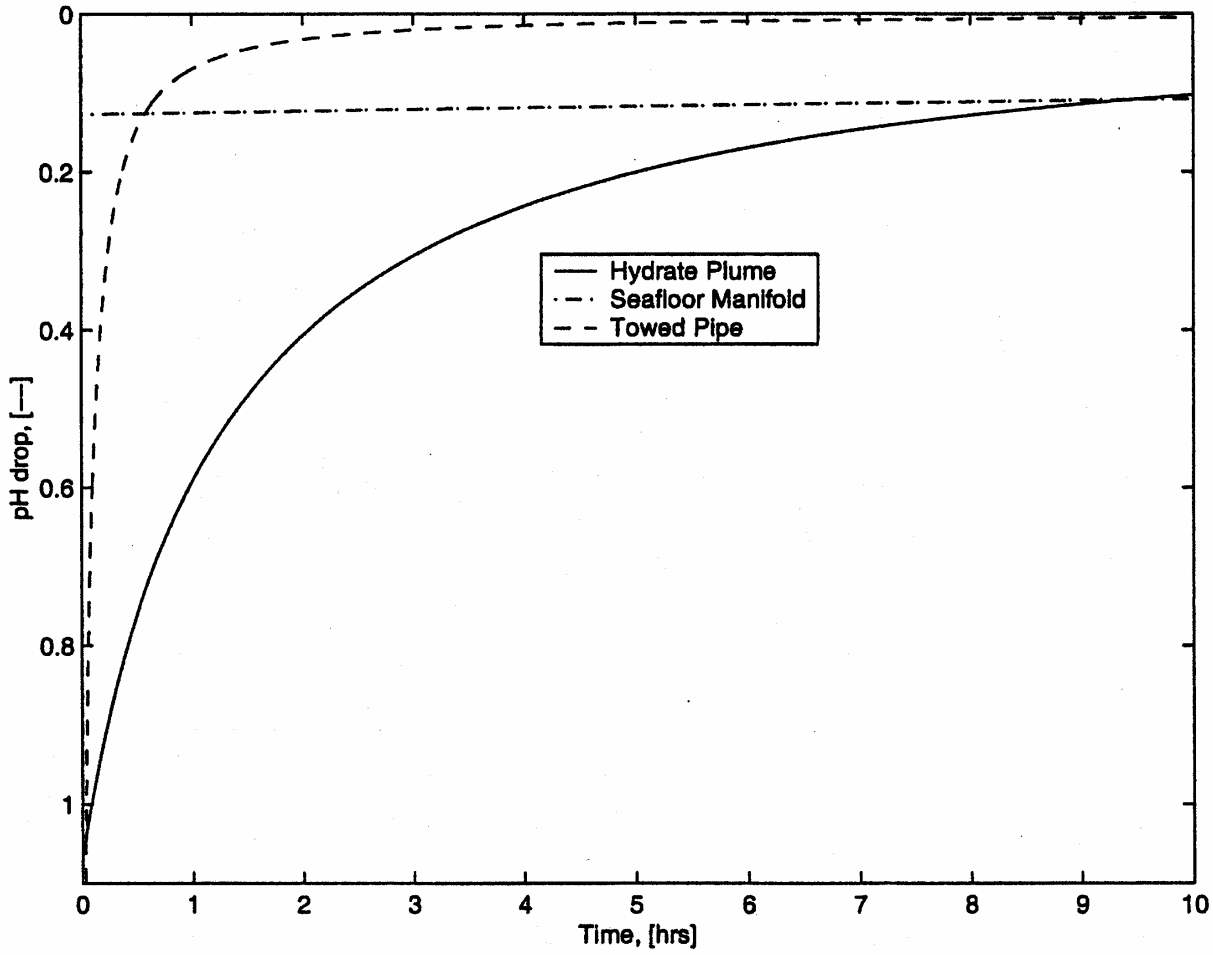

Figure 4 pH drop versus time for three different release scenarios

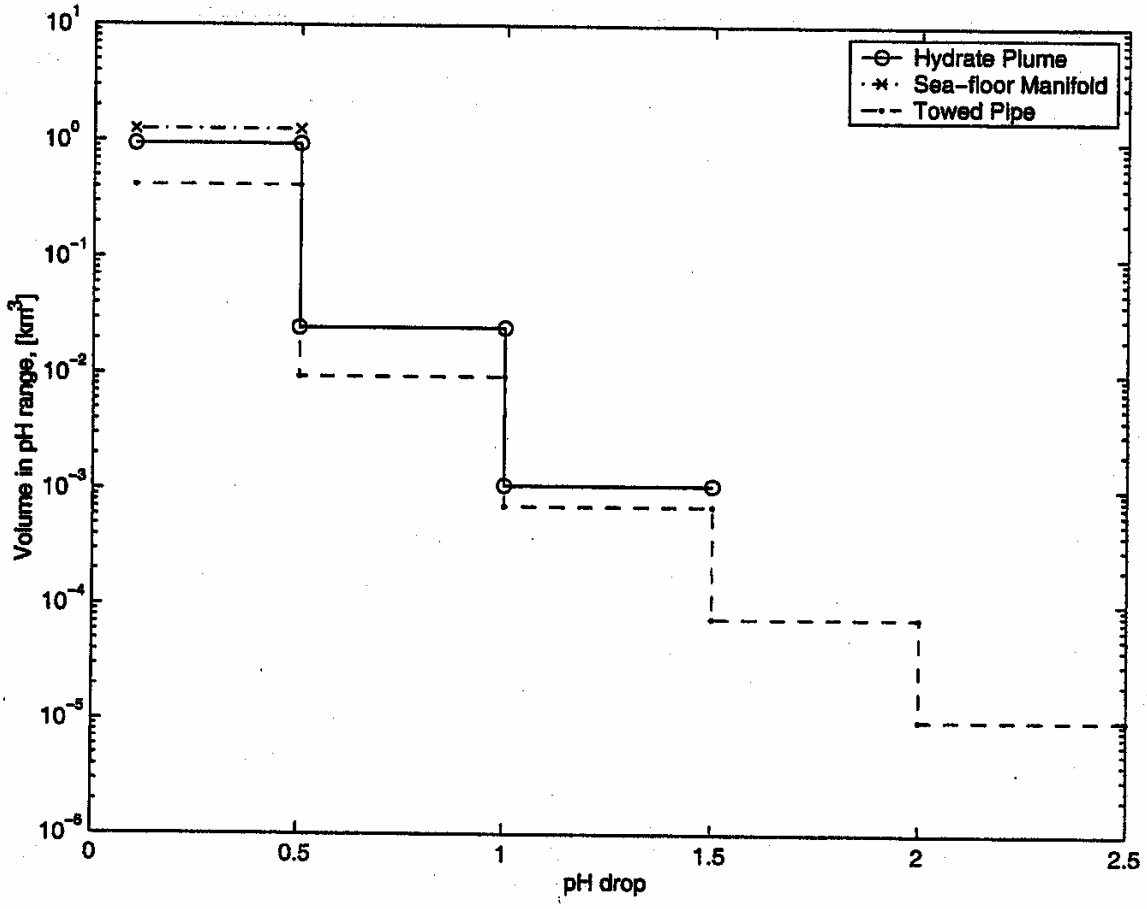

Figure 5 Volume of water contained within different ranges of pH drop for three release scenarios

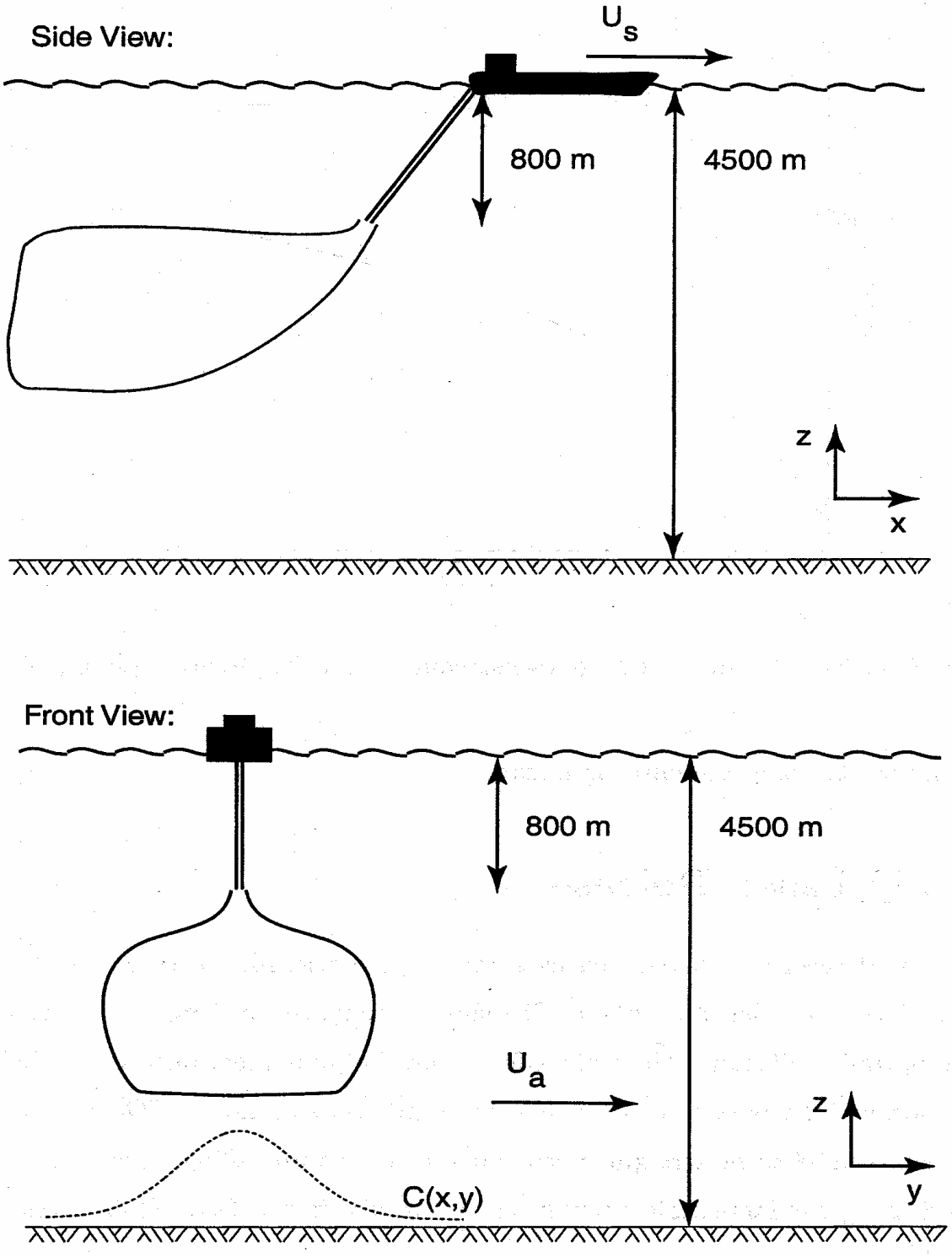

Figure 6 CO_2 hydrate particles released from a moving ship

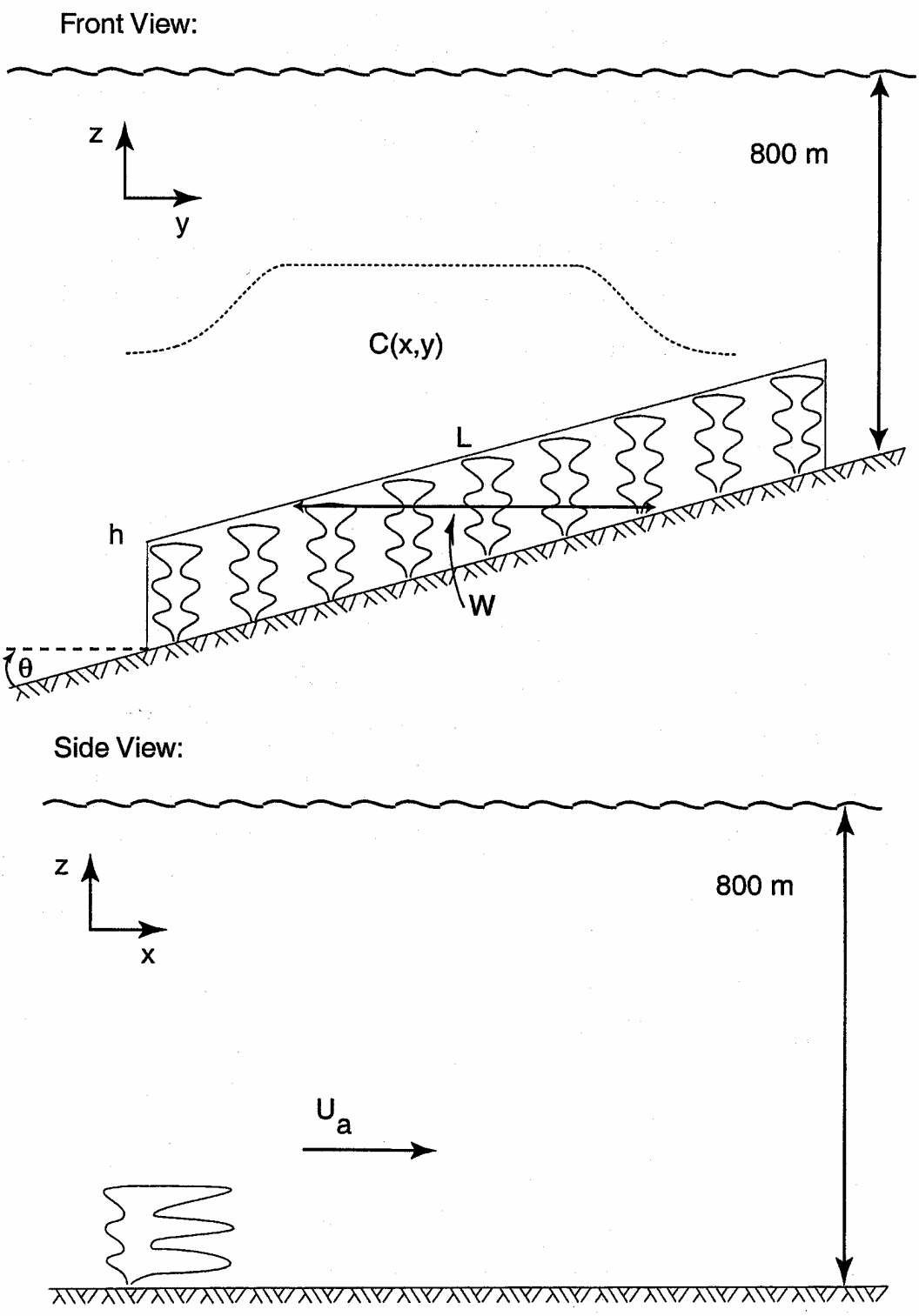

Figure 7 Rising CO_2 droplets released from a bottom manifold

Figure 8 Schematic depiction (not to scale) comparing three injection scenarios. Initial concentration for point source (top) and bottom manifold (bottom) scale in proportion to $\dot{m}/hwu_a$. Initial concentration for moving ship (middle) scale in proportion to $\dot{m}/hwU_s$